Cell Reports, Volume *36*

Supplemental information

The angiopoietin-Tie2 pathway regulates Purkinje cell dendritic morphogenesis in a cell-autonomous manner

Robert Luck, Andromachi Karakatsani, Bhavin Shah, Geza Schermann, Heike Adler, Janina Kupke, Nathalie Tisch, Hyun-Woo Jeong, Michaela Kerstin Back, Florian Hetsch, Anna D'Errico, Michele De Palma, Ellen Wiedtke, Dirk Grimm, Amparo Acker-Palmer, Jakob von Engelhardt, Ralf H. Adams, Hellmut G. Augustin, and Carmen Ruiz de Almodóvar

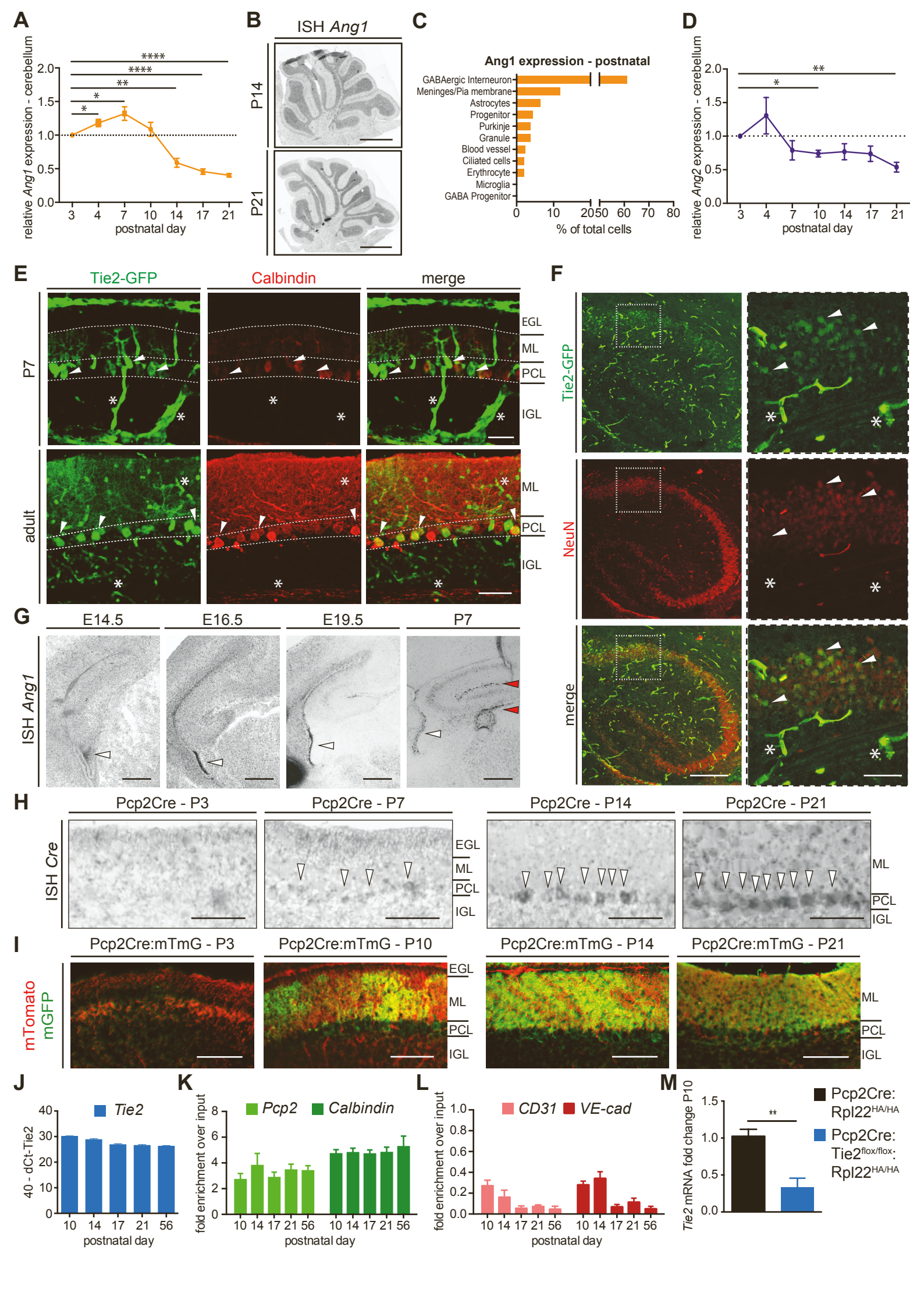
A
relative Ang1 expression - cerebellum
postnatal day
B
ISH Ang1
P14
P21
C
Ang1 expression - postnatal
GABAergic Interneuron
Meninges/Pia membrane
Astrocytes
Progenitor
Purkinje
Granule
Blood vessel
Ciliated cells
Erythrocyte
Microglia
GABA Progenitor
% of total cells
D
relative Ang2 expression - cerebellum
postnatal day
E
Tie2-GFP
Calbindin
merge
P7
adult
EGL
ML
PCL
IGL
F
Tie2-GFP
NeuN
merge
G
E14.5
E16.5
E19.5
P7
ISH Ang1
H
Pcp2Cre - P3
Pcp2Cre - P7
Pcp2Cre - P14
Pcp2Cre - P21
ISH Cre
I
Pcp2Cre:mTmG - P3
Pcp2Cre:mTmG - P10
Pcp2Cre:mTmG - P14
Pcp2Cre:mTmG - P21
mTomato
mGFP
J
Tie2
40 - dCt-Tie2
postnatal day
K
Pcp2
Calbindin
fold enrichment over input
postnatal day
L
CD31
VE-cad
fold enrichment over input
postnatal day
M
Tie2 mRNA fold change P10
Pcp2Cre: Rpl22HA/HA
Pcp2Cre: Tie2flox/flox: Rpl22HA/HA

Figure S1. Ang1, Ang2 and Tie2 are dynamically expressed in the mouse cerebellum during postnatal development. Related to Figure 1. A) mRNA expression of *Ang1* was analyzed by qPCR in RNA from whole cerebellar lysates at different postnatal stages. Data are represented as mean±SEM from n=6 animals. Data are not significant if not indicated. One sample t-test; *p<0.05; **p<0.01; ****p<0.0001. B) Representative images of the sense probe for *Ang1* mRNA ISH in cerebellar sections of P14 and P21 (overview pictures on top; images of insets below). Scale bar 1mm (top) or 500µm (bottom). C) Ang1 expression was analyzed from an available single-cell RNA sequencing data set of the developing murine cerebellum (Carter et al., 2018). Shown is the percentage of total annotated cells. D) mRNA expression of *Ang2* was analyzed by qPCR in RNA from whole cerebellar lysates at different postnatal stages. Data are represented as mean±SEM from n=6 animals. Data are not significant if not indicated. One sample t-test; *p<0.05; **p<0.01. E) Representative image of cerebellar tissue of P7 Tie2-GFP mice stained for GFP and Calbindin (PC marker). Double-positive cells are indicated with white arrowhead. Asterisks shows GFP-positive blood vessels.Scale bar 50µm. F) Representative images of the hippocampus of Tie2-GFP mice (P9) were stained for GFP and the neuronal-marker NeuN. Double-positive cells are indicated with white arrows and GFP-positive blood vessels with asterisk. Insets of left panels are shown at higher magnification in the right panels. Images are shown on the left. Scale bar: left: 100µm; right: 50µm. G) Representative images of ISH for *Ang1* on mouse hippocampal sections of different embryonic and postnatal stages. White arrowheads indicate positive staining adjacent to the fimbria, while red arrowheads show *Ang1* mRNA signal in cells around the dentate gyrus. Scale bar 100µm. H) Representative images of ISH for *Cre* mRNA on cerebella sections at different postnatal stages. White arrowheads show Cre+ mRNA PCs. Scale bar 100µm. I) Representative images of cerebella sections from Pcp2Cre:mT/mG at different postnatal stages. Scale bar 100µm. J) Quantification of *Tie2* mRNA expression in isolated ribosome bound mRNA purified from PCs ribosomes of Pcp2Cre:Rpl22$^{+/HA}$ mice at different postnatal stages. *Tie2* mRNA levels are shown as 40 – dCt-Tie2. Data are represented as mean±SEM from a minimum of n=4 animals. K, L) The enrichment of PC-specific genes *Pcp2* and *Calbindin* (K) as well as the decline of endothelial-specific genes *CD31* and *VE-Cadherin* (L) was analyzed to show the functionality of the method. Data are represented as mean±SEM from a minimum of n=3 animals. M) Quantification of *Tie2* mRNA expression in isolated ribosome-bound mRNA purified from PCs ribosomes of Pcp2Cre:Rpl22$^{HA/HA}$ or Pcp2Cre:Tie2$^{flox/flox}$:Rpl22$^{HA/HA}$ animals at P10 showing a reduction of Tie2 expression in Pcp2Cre:Tie2$^{flox/flox}$:Rpl22$^{HA/HA}$ mice. Results were normalized to the Pcp2Cre:Rpl22$^{HA/HA}$ animals. Data are represented as mean±SEM from a minimum of n=4 animals. Unpaired Student's t-test; **p<0.01.

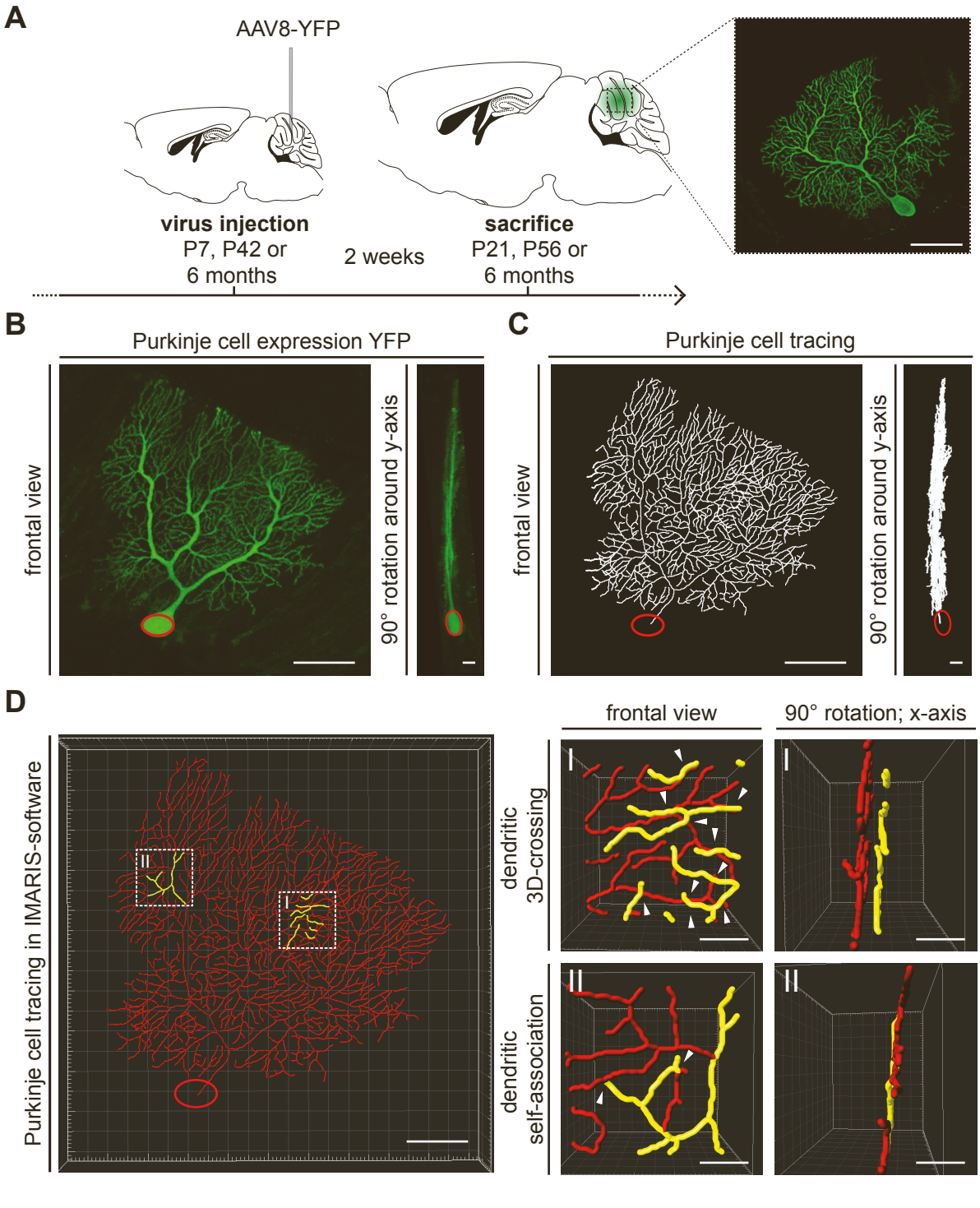
A
AAV8-YFP
virus injection
P7, P42 or
6 months
2 weeks
sacrifice
P21, P56 or
6 months
B
Purkinje cell expression YFP
frontal view
90° rotation around y-axis
C
Purkinje cell tracing
frontal view
90° rotation around y-axis
D
Purkinje cell tracing in IMARIS-software
frontal view
90° rotation; x-axis
dendritic
3D-crossing
dendritic
self-association
I
II

Figure S2. Schematic workflow of PC dendritic analysis. Related to STAR Methods. A) Injection protocol used to label single PCs for later dendritic reconstruction. AAV8-YFP was injected into the cerebellum of mice at the age of P7, P42 and 6 months. Animals were sacrificed for analysis after 2 weeks at P21, P56 or 6 months. Scale bar 50µm. Images adapted from 'The Mouse Brain in Stereotaxic Coordinates'; Academic Press 2001. B, C) Confocal Z-stack images were taken from YFP-expression PCs (B) and dendritic morphology was manually traced using FIJI plugin 'Simple Neurite Tracer' (C). Left panels show the frontal view (scale bar 50 µm); right panels show a 90° rotated side view (scale bar 10 µm). D) IMARIS software was used to perform additional analysis on the 3D-structure of PC dendrites. Left panel shows the 3D-view of the PC dendrites in red (scale bar 50 µm). Two areas are magnified on the right. Yellow and red traces show dendritic crossing, which is further highlighted with white arrowheads. In the analysis, it was differentiated whether the dendritic crossing is due to a 3D-overlap (I) or due to dendritic self-association (II). Scale bar 10 µm.

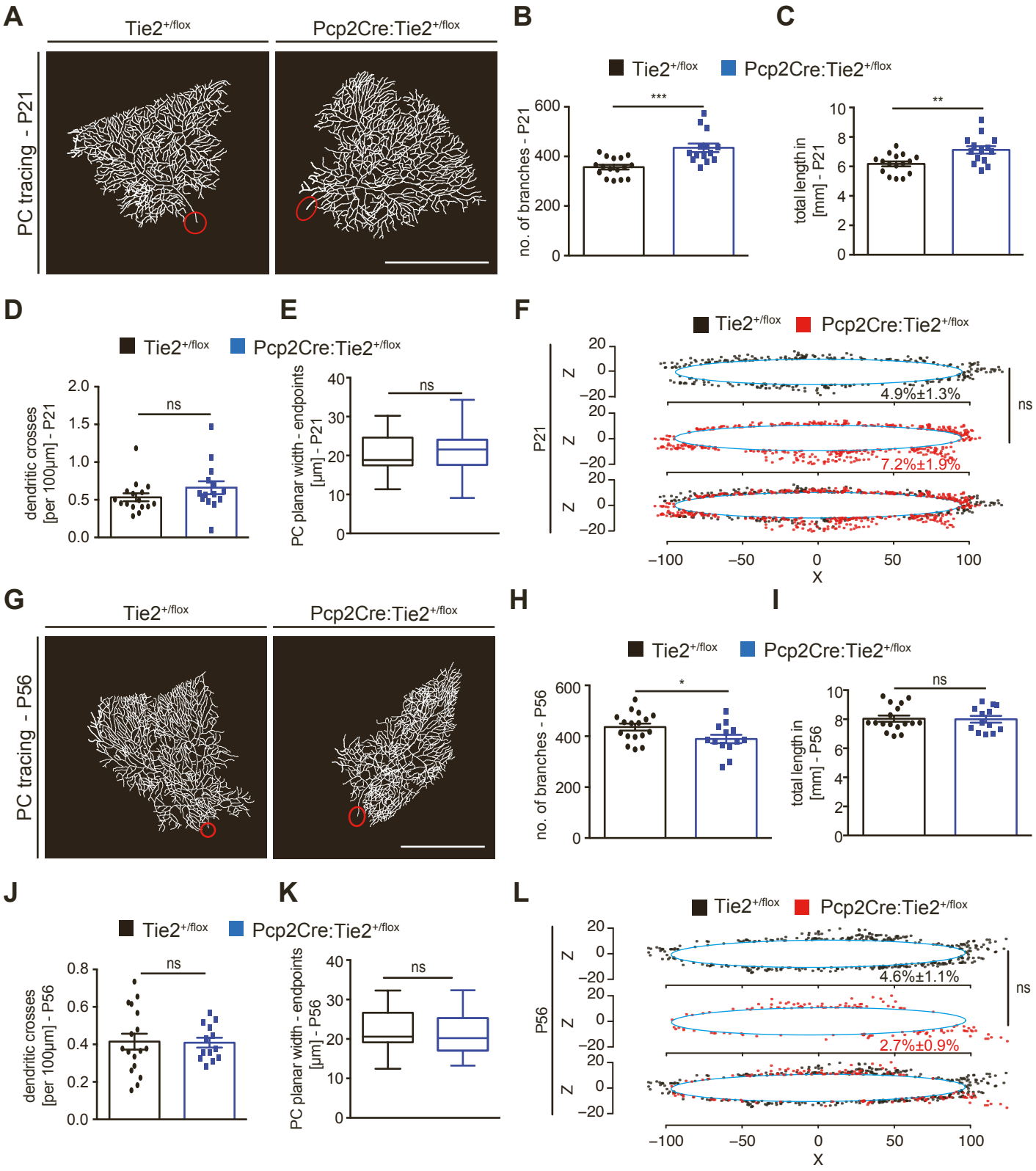
A
Tie2+/flox
Pcp2Cre:Tie2+/flox
PC tracing - P21
B
C
Tie2+/flox
Pcp2Cre:Tie2+/flox
***
**
no. of branches - P21
total length in [mm] - P21
D
E
F
Tie2+/flox
Pcp2Cre:Tie2+/flox
ns
dendritic crosses [per 100µm] - P21
PC planar width - endpoints [µm] - P21
P21
4.9%±1.3%
7.2%±1.9%
X
G
Tie2+/flox
Pcp2Cre:Tie2+/flox
PC tracing - P56
H
I
*
ns
no. of branches - P56
total length in [mm] - P56
J
K
L
dendritic crosses [per 100µm] - P56
PC planar width - endpoints [µm] - P56
P56
4.6%±1.1%
2.7%±0.9%

Figure S3. Pcp2Cre:Tie2$^{+/flox}$ animals resemble the dendritic phenotype observed in Pcp2Cre:Tie2$^{flox/flox}$ mice. Related to Figure 2 and Figure 3. A-L) Dendritic properties were analyzed in Tie2$^{+/flox}$ and Pcp2Cre:Tie2$^{+/flox}$ mice at P21 (A-F) and P56 (G-L). Representative traced PCs of Tie2$^{+/flox}$ and Pcp2Cre:Tie2$^{+/flox}$ mice are shown in A and G. Scale bar 50µm. Quantification of the number of branches (B, H) and total dendritic length (C, I). Quantification of dendritic crosses (defined points were PC dendrites cross and touch each other) in Tie2$^{+/flox}$ and Pcp2Cre:Tie2$^{+/flox}$ mice (D, J). Data are shown as mean±SEM from a minimum of n=13 neurons from a minimum of 4 independent animals. E, K) Quantification of PC planarity in Tie2$^{+/flox}$ and Pcp2Cre:Tie2$^{+/flox}$ mice. Data are represented as boxplot with whiskers showing minimum and maximum values from a minimum of n=13 neurons from a minimum of two independent animals. F, L) An ellipse (shown in light blue) of the 95-percentile density distribution of all endpoints was quantified using the pool of control animals (upper graphs). This ellipse was then fitted onto the Pcp2Cre:Tie2$^{+/flox}$ animals (middle graphs). Merged graphs for each mouse line and time point are shown in the lower panels. The percentage of branch endpoints outside the ellipse was calculated for each image and the mean±SD is depicted from a minimum of n=13 neurons from a minimum of two independent animals. Unpaired Student's t-test; **p<0.01; ***p<0.001; ns=not significant.

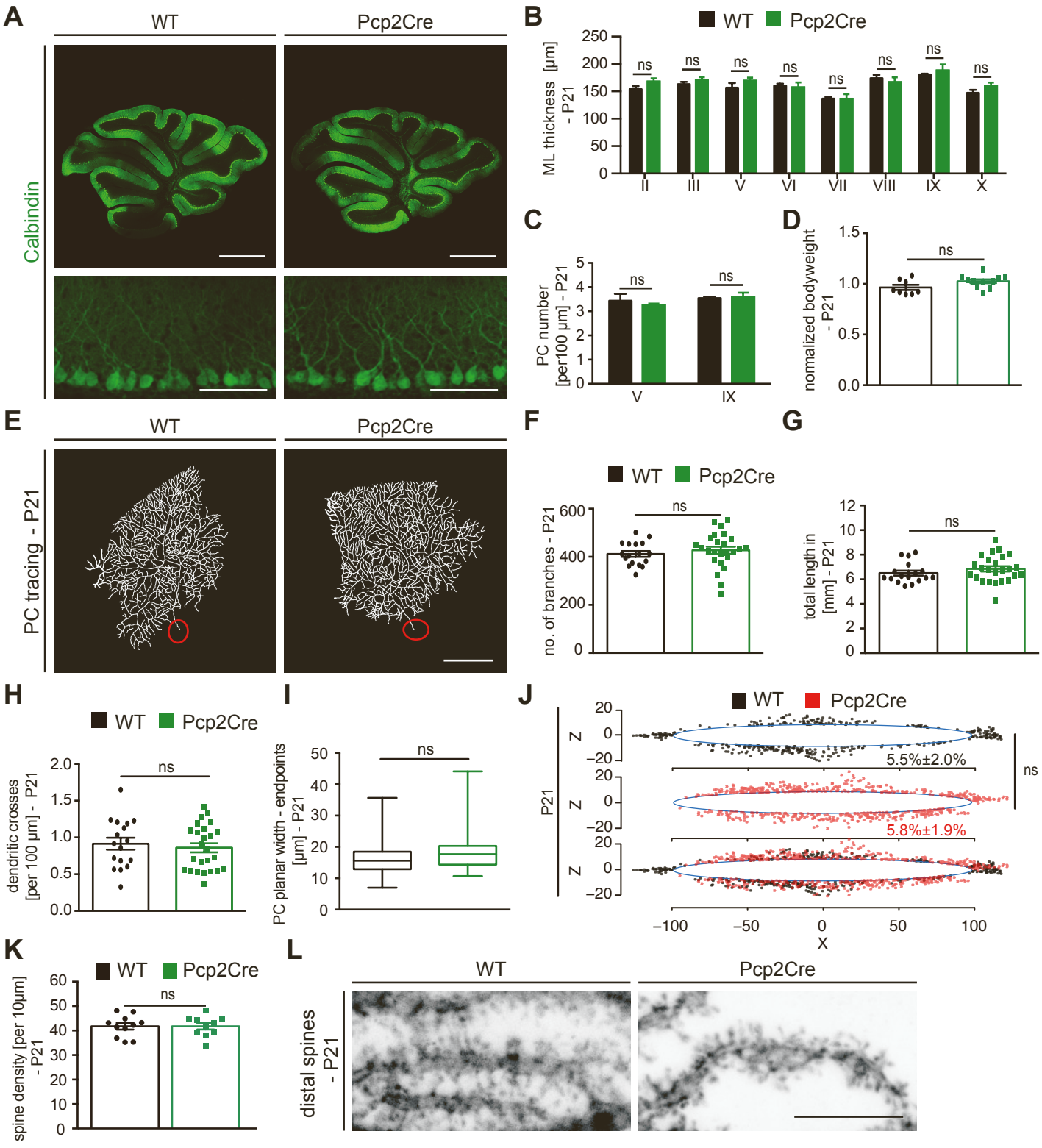
A
WT
Pcp2Cre
Calbindin
B
WT
Pcp2Cre
ML thickness [µm] - P21
250
200
150
100
50
0
ns
II
III
V
VI
VII
VIII
IX
X
C
PC number [per100 µm] - P21
5
4
3
2
1
0
ns
V
IX
D
normalized bodyweight - P21
1.5
1.0
0.5
0.0
ns
E
WT
Pcp2Cre
PC tracing - P21
F
WT
Pcp2Cre
no. of branches - P21
600
400
200
0
ns
G
total length in [mm] - P21
12
10
8
6
4
2
0
ns
H
WT
Pcp2Cre
dendritic crosses [per 100 µm] - P21
2.0
1.5
1.0
0.5
0.0
ns
I
PC planar width - endpoints [µm] - P21
50
40
30
20
10
0
ns
J
WT
Pcp2Cre
P21
Z
20
0
−20
5.5%±2.0%
5.8%±1.9%
ns
−100
−50
0
50
100
X
K
WT
Pcp2Cre
spine density [per 10µm] - P21
60
50
40
30
20
10
0
ns
L
WT
Pcp2Cre
distal spines - P21

Figure S4. Pcp2-specific Cre expression in PCs does not show any PC dendritic morphogenesis abnormality. Related to Figure 2, Figure 3 and Figure 6. A) Representative images of WT and Pcp2Cre cerebella sections at P21 stained with Calbindin (PC marker). Scale bar: higher panels: 1mm; lower panels; 100µm. B) Bar graph showing ML thickness at P21 in all cerebella lobes (II-X). C) Bar graph showing PC number per 100µm in lobes V and IX. Data shown as mean±SEM from a minimum of n=3 animals per genotype. Unpaired Student's t-test for each lobe. D) Bar graph showing normalized bodyweight of WT and Pcp2Cre P21 mice (minimum of 8 mice per genotype). E) Representative traced PCs of WT and Pcp2Cre mice at P21. Scale bar 50µm. F-H) Quantification of the number of branches (F) and total dendritic length (G) at P21. Quantification of dendritic crosses (H) (defined points were PC dendrites cross and touch each other) in WT and Pcp2Cre P21 mice. Data are shown as mean±SEM from a minimum of n=17 neurons from a minimum of five independent animals. I) Quantification of PC planarity in WT and Pcp2Cre mice at P21. Data are represented as boxplot with whiskers showing minimum and maximum values from a minimum of n=17 neurons from a minimum of 5 independent animals. J) An ellipse (shown in light blue) of the 95-percentile density distribution of all endpoints was quantified using the pool of control animals (upper graphs). This ellipse was then fitted onto the WT animals (middle graphs). Merged graphs for each mouse line and time point are shown in the lower panels. The percentage of branch endpoints outside the ellipse was calculated for each image and the mean±SD is depicted from a minimum of n=17 neurons from a minimum of five independent animals. Unpaired Student's t-test; ns=not significant. K, L) Distal dendritic spines were counted in AAV8-transduce PCs in WT and Pcp2Cre animals at P21. Data are represented as mean±SEM from a minimum of n=10 neurons from a minimum of three independent animals. Unpaired Student's t-test; ns=not significant. Representative pictures are shown in L. Scale bar 5µm.

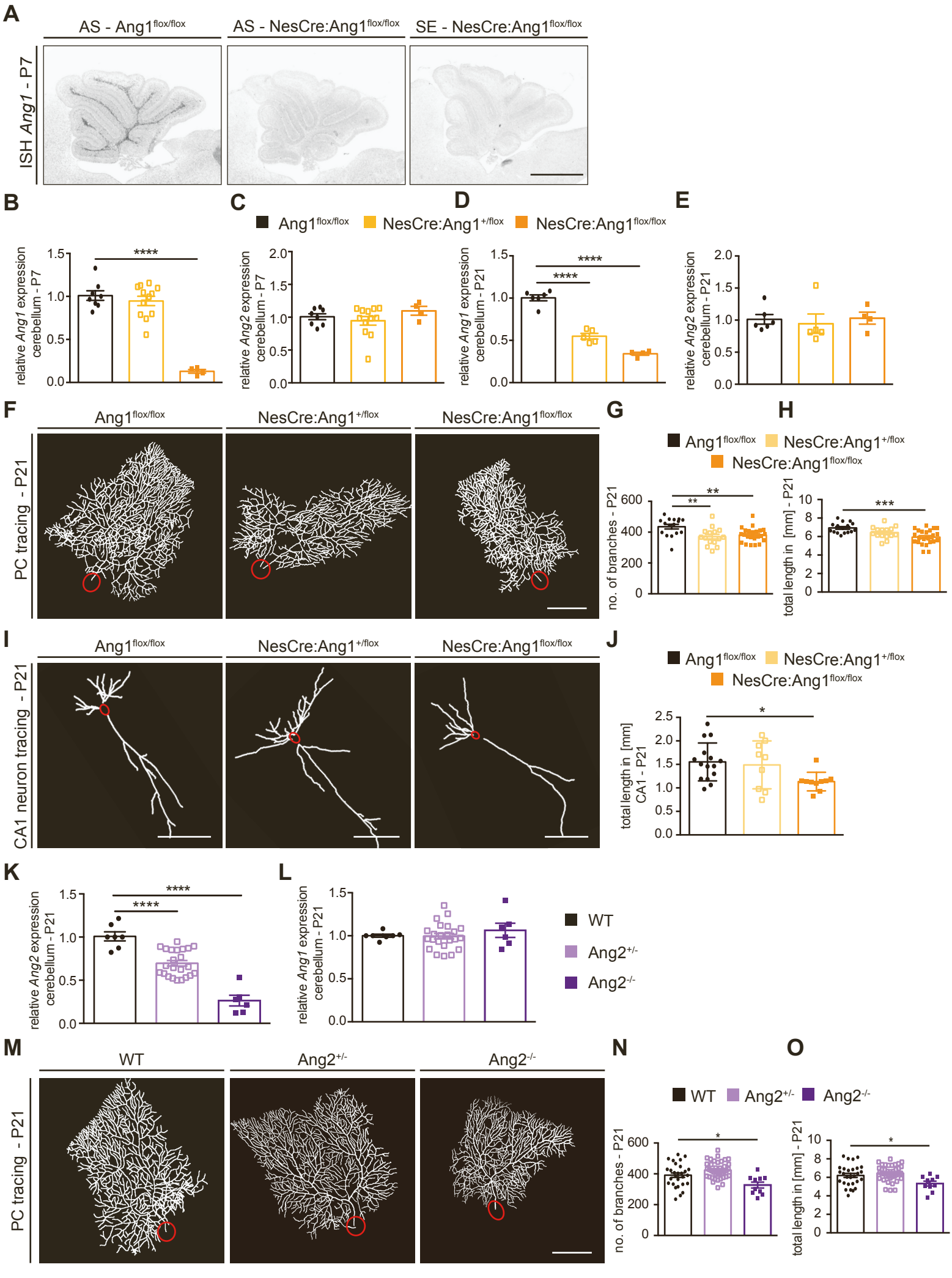
A
AS - Ang1flox/flox
AS - NesCre:Ang1flox/flox
SE - NesCre:Ang1flox/flox
ISH Ang1 - P7
B
C
D
E
Ang1flox/flox
NesCre:Ang1+/flox
NesCre:Ang1flox/flox
relative Ang1 expression cerebellum - P7
relative Ang2 expression cerebellum - P7
relative Ang1 expression cerebellum - P21
relative Ang2 expression cerebellum - P21
****
F
G
H
PC tracing - P21
no. of branches - P21
total length in [mm] - P21
**
***
I
J
CA1 neuron tracing - P21
total length in [mm] CA1 - P21
*
K
L
WT
Ang2+/-
Ang2-/-
M
N
O
PC tracing - P21
no. of branches - P21
total length in [mm] - P21

Figure S5. NesCre:Ang1$^{flox/flox}$ and Ang2-deficient mice present defects in dendritic branching of PCs and hippocampal neurons. Related to Figure 3. A) ISH of *Ang1* mRNA in P7 cerebella sections of the indicated mice. Shown are antisense (AS) and sense (SE) probes. Scale bar 1mm. B-E) Quantification of *Ang1* and *Ang2* mRNA expression in total RNA isolated from cerebella of P7 (B, C) and P21 (D, E) animals. Values are normalized to the Cre-negative animals from the same litter. Data are represented as mean±SEM from a minimum of n=4 animals. Data are not significant if not indicated. One-way ANOVA; ****p<0.0001. F) Representative traced PCs of Ang1$^{flox/flox}$, NesCre:Ang1$^{+/flox}$ and NesCre:Ang1$^{flox/flox}$ at P21. Scale bar 50µm. G, H) Quantification of the number of branches (G) and total dendritic length (H) at P21. Data are represented as mean±SEM from a minimum of n=16 neurons from a minimum of 3 independent animals. Data are not significant if not indicated. One-way ANOVA; **p<0.01; ***p<0.001. I) Representative traced Golgi-stained CA1 hippocampal neurons at P21 for the indicated mice. Scale bar 100µm. J) Quantification of total dendritic length of CA1 hippcampal neurons of the indicated mice at P21. Data are represented as mean±SEM from a minimum of n=9 neurons from a minimum of 3 independent animals. Data are not significant if not indicated. One-way ANOVA; *p<0.05. K, L) Quantification of *Ang1* and *Ang2* mRNA expression in total RNA isolated from cerebella of P21 mice. Data is normalized to the WT animals of the litter. Data are represented as mean±SEM from a minimum of n=6 animals. Data are not significant if not indicated. One-way ANOVA; ****p<0.0001. M) Representative traced PCs of WT, Ang2$^{+/-}$ and Ang2$^{-/-}$ mice at P21. Scale bar 50µm N, O) Quantification of the number of branches (N) and total dendritic length (O) at P21. Data are represented as mean±SEM from a minimum of n=10 neurons from a minimum of three independent animals. Data are not significant if not indicated. One-way ANOVA; *p<0.05.

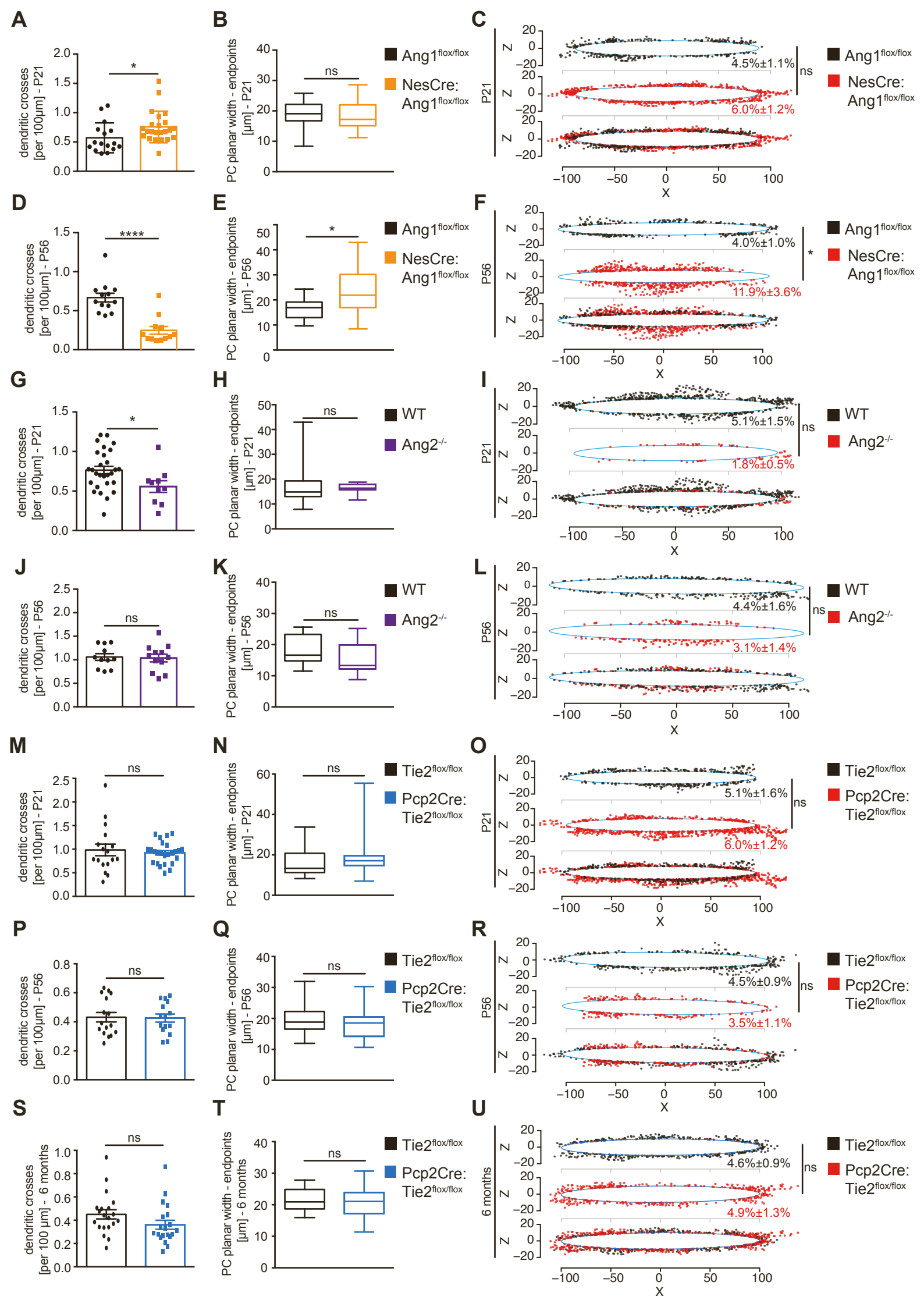
A
dendritic crosses [per 100µm] - P21
*
B
PC planar width - endpoints [µm] - P21
ns
Ang1flox/flox
NesCre: Ang1flox/flox
C
P21
4.5%±1.1%
6.0%±1.2%
ns
X
D
dendritic crosses [per 100µm] - P56
****
E
PC planar width - endpoints [µm] - P56
*
F
P56
4.0%±1.0%
11.9%±3.6%
*
G
dendritic crosses [per 100µm] - P21
*
H
PC planar width - endpoints [µm] - P21
ns
WT
Ang2-/-
I
P21
5.1%±1.5%
1.8%±0.5%
ns
J
dendritic crosses [per 100µm] - P56
ns
K
PC planar width - endpoints [µm] - P56
ns
L
P56
4.4%±1.6%
3.1%±1.4%
ns
M
dendritic crosses [per 100µm] - P21
ns
N
PC planar width - endpoints [µm] - P21
ns
Tie2flox/flox
Pcp2Cre: Tie2flox/flox
O
P21
5.1%±1.6%
6.0%±1.2%
ns
P
dendritic crosses [per 100µm] - P56
ns
Q
PC planar width - endpoints [µm] - P56
ns
R
P56
4.5%±0.9%
3.5%±1.1%
ns
S
dendritic crosses [per 100 µm] - 6 months
ns
T
PC planar width - endpoints [µm] - 6 months
ns
U
6 months
4.6%±0.9%
4.9%±1.3%
ns

Figure S6. NesCre:Ang1$^{flox/flox}$, Ang2-deficient and Pcp2Cre:Tie2$^{flox/flox}$ mice show changes in dendritic self-avoidance and planarity. Related to Figure 2 and Figure 3. A-F) Dendritic properties were analyzed in Ang1$^{flox/flox}$ and NesCre:Ang1$^{flox/flox}$ animals at P21 (A-C) and P56 (D-F). Quantification of dendritic crosses (defined points were PC dendrites cross and touch each other) are shown in (A, D). Data are shown as mean±SEM from a minimum of n=11 neurons from a minimum of three independent animals. Quantification of PC planarity is shown in (B, E). Data are represented as boxplot with whiskers showing minimum and maximum values for a minimum of n=11 neurons from a minimum of three independent animals. An ellipse (shown in light blue) of the 95-percentile density distribution of all endpoints was quantified using the pool of control animals (upper graphs). This ellipse was then fitted onto the Ang1$^{flox/flox}$ animals (middle graphs). Merged graphs for each mouse line and time point are shown in the lower panels (C, F). The percentage of branch endpoints outside the ellipse was calculated for each image and the mean±SD is depicted from a minimum of n=11 neurons for a minimum of three independent animals. Unpaired Student's t-test; *p<0.05; ****p<0.0001; ns=not significant. G-L) Dendritic properties were analyzed in WT and Ang2$^{-/-}$ animals at P21 (G-I) and P56 (J-L). Quantification of dendritic crosses (defined points were PC dendrites cross and touch each other) are shown in (G, J).Data are shown as mean±SEM for a minimum of n=10 neurons from a minimum of three independent animals. Quantification of PC planarity is shown in (H, K). Data are represented as boxplot with whiskers showing minimum and maximum values for a minimum of n=10 neurons from a minimum of three independent animals. An ellipse (shown in light blue) of the 95-percentile density distribution of all endpoints was quantified using the pool of control animals (upper graphs). This ellipse was then fitted onto the WT animals (middle graphs). Merged graphs for each mouse line and time point are shown in the lower panels (I, L). The percentage of branch endpoints outside the ellipse was calculated for each image and the mean±SD is depicted from a minimum of n=10 neurons from a minimum of 3 independent animals. Unpaired Student's t-test; *p<0.05; ns=not significant. M-U) Dendritic properties were analyzed in Tie2$^{flox/flox}$ and Pcp2Cre:Tie2$^{flox/flox}$ animals at P21 (M-O), P56 (P-R) and 6 months (S-U). Quantification of dendritic crosses (defined points where PC dendrites cross and touch each other) are shown in (M, P, S). Data are shown as mean±SEM from a minimum of n=15 neurons from a minimum of three independent animals. Quantification of PC planarity is shown in (N, Q, T). Data are represented as box plot with whiskers showing minimum and maximum values from a minimum of n=15 neurons from a minimum of three independent animals. An ellipse (shown in light blue) of the 95-percentile density distribution of all endpoints was quantified using the pool of control animals (upper graphs). This ellipse was then fitted onto the Pcp2Cre:Tie2$^{flox/flox}$ animals (middle graphs). Merged graphs for each mouse line and time point are shown in the lower panels (O, R, U). The percentage of branch endpoints outside the ellipse was calculated for each image and the mean±SD is depicted from a minimum of n=15 neurons from a minimum of 3 independent animals. Unpaired Student's t-test; ns=not significant.

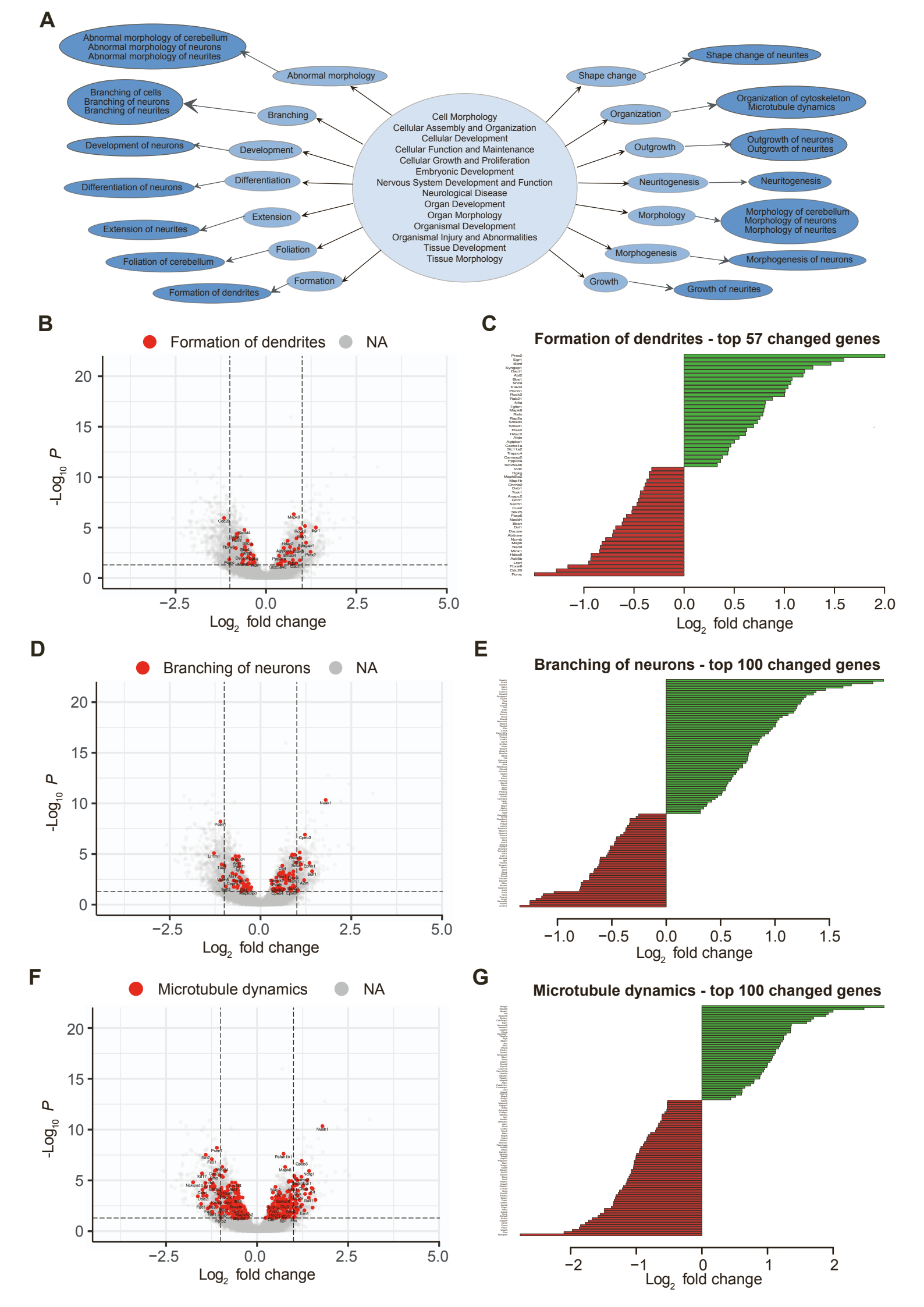
A
Abnormal morphology of cerebellum
Abnormal morphology of neurons
Abnormal morphology of neurites
Abnormal morphology
Branching of cells
Branching of neurons
Branching of neurites
Branching
Development of neurons
Development
Differentiation of neurons
Differentiation
Extension of neurites
Extension
Foliation of cerebellum
Foliation
Formation of dendrites
Formation
Cell Morphology
Cellular Assembly and Organization
Cellular Development
Cellular Function and Maintenance
Cellular Growth and Proliferation
Embryonic Development
Nervous System Development and Function
Neurological Disease
Organ Development
Organ Morphology
Organismal Development
Organismal Injury and Abnormalities
Tissue Development
Tissue Morphology
Shape change
Shape change of neurites
Organization
Organization of cytoskeleton
Microtubule dynamics
Outgrowth
Outgrowth of neurons
Outgrowth of neurites
Neuritogenesis
Neuritogenesis
Morphology
Morphology of cerebellum
Morphology of neurons
Morphology of neurites
Morphogenesis
Morphogenesis of neurons
Growth
Growth of neurites
B
Formation of dendrites
NA
-Log10 P
Log2 fold change
C
Formation of dendrites - top 57 changed genes
Log2 fold change
D
Branching of neurons
NA
-Log10 P
Log2 fold change
E
Branching of neurons - top 100 changed genes
Log2 fold change
F
Microtubule dynamics
NA
-Log10 P
Log2 fold change
G
Microtubule dynamics - top 100 changed genes
Log2 fold change

Figure S7. PC-specific loss of Tie2 leads to alterations in the expression of genes involved in neuronal wiring. Related to Figure 5. A) Ribosome bound mRNA was purified from PCs ribosomes of Pcp2Cre:Rpl22$^{HA/HA}$ or Pcp2Cre:Tie2$^{flox/flox}$:Rpl22$^{HA/HA}$ animals at P56 and sent for sequencing. Changes in gene expression were analyzed with Ingenuity Pathway Analysis (IPA). Annotated groups and subgroups are shown. B-G) Among annotations, 'Formation of dendrites' (B, C), 'Branching of neurons' (D, E) and 'Microtubule dynamics' (F, G) are shown. Total gene changes (lfcShrink fold change) are visualized by volcano-plot in B, D and F. The top 100 up- and down-regulated genes of the annotations are shown ranked by unmodified log2 fold-change in C, E and G.